Shape Persistence and Bistability of Planar Three-Fold Core Polyphenylene Dendrimers: A Molecular Dynamics Study

Paola Carbone,[†,‡] Aurora Calabretta,[†] Marco Di Stefano,[†] Fabrizia Negri,*[,†,‡] and Klaus Müllen[§]

Dipartimento di Chimica "G. Ciamician", Università di Bologna, Via Francesco Selmi 2, 40126 Bologna, Italy, INSTM UdR Bologna, Italy, and Max-Planck-Institut für Polymerforschung, Ackermannweg 10, D-55128 Mainz, Germany

Received: September 12, 2005; In Final Form: December 15, 2005

We present an atomistic molecular dynamics investigation of the structural time evolution of isolated polyphenylene dendrimers, carbon based dendrimers with a planar core formed by a 1,3,5 trisubstituted benzene ring. Simulations are carried out at low (80 K) and room temperature. A general classification of the conformations (core conformations) assumed by the three dendrimer branches with respect to the planar core is presented. It is found that out of the six possible core conformations only four are stable, the remaining two being unstable for steric reasons. For second generation dendrimers, two of the four accessible core conformations are associated with an *open* arrangement of the three branches attached to the planar 3-fold core of the dendrimer, whereas the remaining two are associated with a *collapsed* arrangement of two branches. At low temperature the initial conformation is generally conserved whereas at room temperature jumps among the four possible core conformations are observed in the nanosecond time range. For second generation dendrimers the core conformation jumps are associated with an oscillation between two global shape states: open and collapsed. The computed bistability of the global shape suggests additional possible functional uses for some of these carbon based dendrimers.

1. Introduction

Dendrimers represent a new class of functional materials and for this reason are attracting increasing attention.[1] Owing to their highly branched, regular structures, they have been used in large variety of applications such as catalysts,[2] as energy or charge-transfer systems,[3−5] for charge transport or light emitting layers in organic light emitting diodes (OLEDs)[6] or even as a template for the preparation of monodisperse metal nanoparticles.[7] Dendrimers tend to adopt a spherical shape for higher generations.[8] Their three-dimensional shape, however, is determined by the core, the building blocks and the surface groups.

Recently, a new class of dendritic systems, composed only of carbon and hydrogen atoms, has been synthesized.[9] Starting from polyfunctional central building blocks, a generation by generation buildup of structurally defined, highly branched polyphenylene dendrimers (PDs) has become possible.[9−11] Among other uses, these dendrimers are employed as precursors in the synthesis of well-defined polycyclic aromatic hydrocarbons (PAHs),[12−15] from which more complex supramolecular structures, such as liquid crystals, can be obtained. PDs are synthesized by cycloaddition of the branching units such as a 3,4-bis(4-[(triisopropylsilyl)ethynyl]phenyl)-2,5-diphenylcyclopenta-2,4-dienone to a multiethynyl substituted core. The core can be, e.g., a 1,3,5 trisubstituted benzene (namely a 3-fold, planar core) or a tetrasubstituted biphenyl or a tetrasubstituted tetraphenylmethane (both are 4-fold, nonplanar cores). Due to their semirigid framework and very dense intramolecular packing, the monodisperse PDs are of interest with respect to the design of nanostructures with invariant shape.[16] Besides their significantly enhanced thermal and chemical stability, their rigidity as compared to aliphatic dendrimer systems, coupled with the wide variety of possible functionalizations, provide the basis for a wide range of potential applications. In this sense, the global shape and the extent of flexibility are important features for the design of well-defined architectures.

Recently, molecular mechanics and molecular dynamics investigations have been reported to study the nature of stable conformers and the shape persistence of PDs based on different cores.[17−20] In a first study, NVT (T = 300 K) molecular dynamics (MD) simulations were carried out on a G2 dendrimer built around a 4-fold biphenyl core,[17] using the MM2 force field and the CERIUS[2] package[21] and it was found that the dendrimer constituted a shape-persistent molecule. In subsequent studies,[18,19] the conformers of PDs of first (G1) and second (G2) generation, with 3-fold or tetrahedral cores were investigated by employing the Universal force field (UFF).[22] Brocorens et al. investigated the dendrimers equilibrated at 300 K and found that the so-called false-propeller structure of the 3-fold core G1 dendrimers is the most stable conformer. However, for the G2 dendrimer, they found its shape to evolve from an *open, false-propeller* structure to a more compact *club-shape* structure in which two branches have collapsed against each other.[18] The authors suggested also that the small energy difference predicted for the different conformations might allow their efficient interconversion. Furthermore, they showed that dendrimers based on a tetraphenylmethane core have a more pronounced shape persistence than those built on a 1,3,5,trisubstituted benzene core. More recently, NVT molecular dynamics simulations based on the Compass force field[23] were reported [20] for

* Corresponding author. E-mail: fabrizia.negri@unibo.it.
[†] Università di Bologna.
[‡] INSTM UdR Bologna.
[§] Max-Planck-Institut für Polymerforschung.

10.1021/jp0551420 CCC: $33.50
Published on Web 01/21/2006

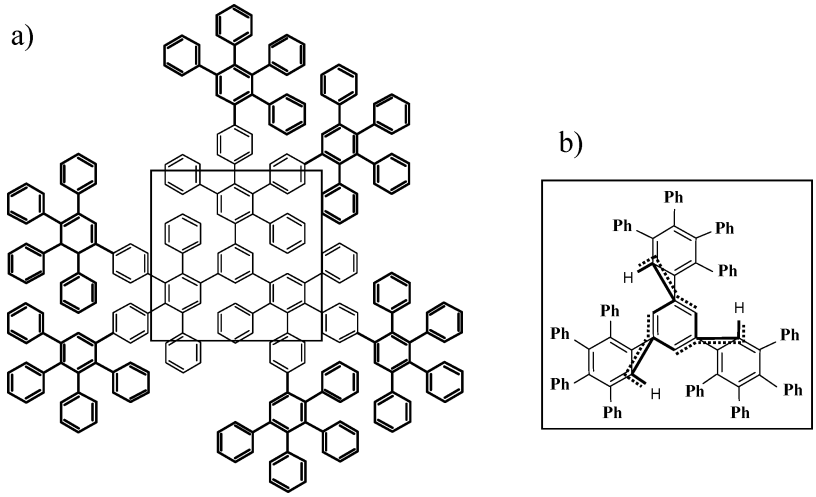

Figure 1. (a) Schematic 2D representation of a planar 3-fold core dendrimer. The thin portions of the branches correspond to the G1 dendrimer. Addition of the thick portions leads to the G2 dendrimer. (b) Core of the dendrimer and a schematic representation of the branches along with the dihedral angles employed to identify the core conformation. Appropriate ranges for these angles are given in the Supporting Information.

the first, second and third generation of PDs built on three different cores, namely planar 3-fold and nonplanar 4-fold. Molecular global shapes and internal organizations as well as molecular surfaces and their implications on the derivatization of PDs were computed. The study revealed, for all the dendrimers investigated, a shape-persistent, nonspherical structure but the deviation from the spherical structure found in ref 20 is more remarkable than that predicted from the simulations of ref 18.

In this work we consider G1 and G2 planar 3-fold core PDs and investigate in greater detail their structural time evolution with the help of longer atomistic molecular dynamics simulations carried out using the MM3 force field.[24] Particular attention is paid to the dynamical evolution of the conformation assumed by the core of the dendrimer and to the associated dendrimer global shape, and a complete classification of the dendrimer's shape in terms of its core conformation is presented. The shape persistence of these and related systems may favor the formation of trapping sites, but the temperature may influence their stability. For this reason we explored the effect of temperature by comparing simulations at low (80 K) and room temperature.

The paper is structured as follows: In section 2 we describe the computational techniques employed for the simulations. In section 3 we describe the core conformations for 3-fold core PDs. In sections 4 and 5 we discuss the simulations carried out on G1 and G2 dendrimers and a conclusion section closes the paper.

2. Computational Details

The G1 and G2 PDs investigated in this work are shown schematically in Figure 1. They are characterized by a planar 3-fold core from which three identical radiating branches emerge. These branches will be labeled blades, in the following, because the overall dendrimer structure resembles a propeller. The blades are composed of the repetitive units, namely by pentaphenyl-substituted benzene rings: one repetitive unit forms the blade of G1 PDs, whereas three of them constitute each blade of G2 PDs.

MD simulations were carried out with the TINKER software[25] and the empirical force field chosen to carry out all the simulations was the MM3 potential,[24] which is particularly well suited to describe conjugated systems, owing to its explicit description of the π-system and through-space interactions between aromatic rings.[26] The most demanding part of the MM3 calculations is the p-electron SCF evaluation of bond orders, required to modify the stretching and torsional parameters of the conjugated bonds. Because bond orders do not change remarkably with the conformation assumed by the dendrimer, we employed the stretching and torsional parameters obtained from energy minimizations and kept them fixed during the subsequent molecular dynamics simulations. This procedure required the definition of two additional atom types for sp^2 carbon atoms (see the Supporting Information), to maintain the appropriate CC bond lengths and flexibility during MD simulations. Notice, indeed, that the CC bond length connecting two phenyl rings is about 1.5 Å, whereas CC bonds in aromatic rings are considerably shorter and stiff (ca. 1.4 Å).

A suitable descriptor of molecular shape is the second moment of the atomic distribution, also known as the gyration tensor which is defined as[27−29] (uniform mass assumed)

$$R_{\alpha,\beta}{}^2 = \frac{1}{N}\sum_{i=1}^{N}(\vec{r}^{\,i}_{\alpha} - \vec{r}^{\,\mathrm{M}}_{\alpha})(\vec{r}^{\,i}_{\beta} - \vec{r}^{\,\mathrm{M}}_{\beta}) \qquad \alpha, \beta = x, y, z$$

where N is the number of atoms in the PDs, $\vec{r}^{\,i}_{\alpha}$ is the position of the ith atom and $\vec{r}^{\,\mathrm{M}}_{\alpha}$ is the position of the dendrimer's center of mass. The above equation allows us to represent the dendrimer in terms of its equivalent ellipsoid, which is a very effective descriptor for compact molecular shapes. Equivalent ellipsoids share characteristic lengths ρ_1, ρ_2 and ρ_3, with the molecules they describe, which are the roots of the eigenvalues[27−29] of the diagonalized gyration tensor:

$$R_{\mathrm{g}}{}^2 = \begin{pmatrix} \rho_1{}^2 & 0 & 0 \\ 0 & \rho_2{}^2 & 0 \\ 0 & 0 & \rho_3{}^2 \end{pmatrix}$$

The squared radius of gyration $R_g{}^2$ is defined as the trace of the tensor, and its average computed over the MD configurations can be compared with experimentally measured radial sizes. We have derived the eigenvalues of the gyration tensor ($\rho_1{}^2$, $\rho_2{}^2$, $\rho_3{}^2$), monitored the time evolution of the characteristic lengths and averaged them over the MD trajectory. The time evolution provides direct indications on the shape's changes whereas the averaged values can be seen as the dimensions of the ellipsoid occupied by the average dendrimer molecule.

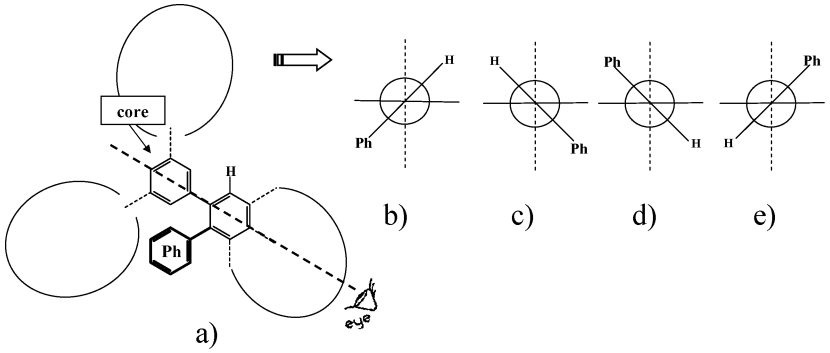

Figure 2. (a) Schematic view of the planar 3-fold core dendrimer with the indication of the phenyl and hydrogen employed to label the reciprocal orientations of pairs of blades. (b)−(e) Newman projections along the direction indicated in (a) showing the four possible orientations of one branch with respect to the dendrimer's core and the positions assumed by the hydrogen and the phenyl group.

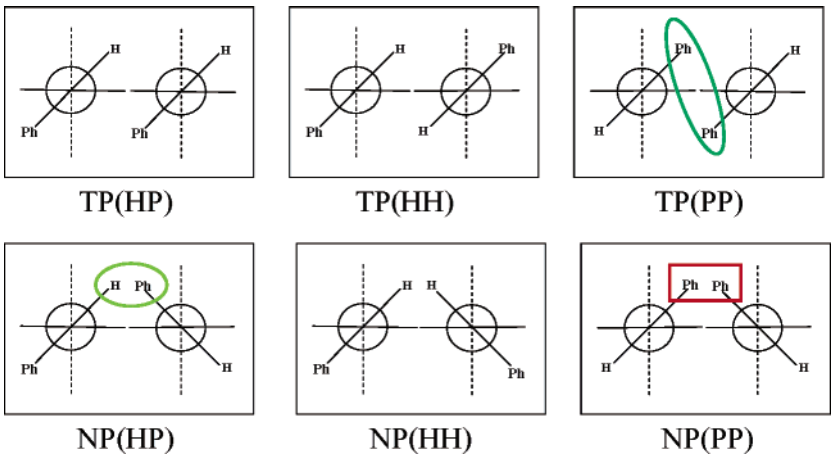

Figure 3. Schematic representation, in terms of Newman projections, and labeling of the six possible reciprocal orientations of the three pairs of branches belonging to planar 3-fold core PDs. Green circles indicate stabilizing interactions; the red rectangle indicates destabilizing interactions.

The G1 and G2 core conformers described in the next section were used to start isothermal NVT MD simulations on isolated dendrimer molecules. Two temperatures were considered, namely 80 and 298 K, to compare the effect of temperature on the dendrimer's shape and core conformational jumps. Simulations at 80 K were 4 ns long, whereas those at room temperature were 8 ns long, and temperature was maintained constant by scaling the velocities via coupling to an external temperature bath using the Berendsen method,[30] with a coupling constant τ_T of 0.1 ps. The van der Waals interactions cutoff was set to 12 Å and the interaction energy beyond the cutoff distance was set to zero for all the simulations. The time step was 1 fs and configurations were saved every 10 ps. Jumps among core conformers were identified by monitoring the time evolution of the three pairs of dihedral angles indicated in the inset of Figure 1 and discussed in the next section (see also the Supporting Information), each pair identifying the reciprocal orientation of two blades.

3. Core Conformations and Initial Structures for MD Simulations

Owing to the torsional flexibility of the phenyl rings, a large number of conformational states can be expected for these PDs, as shown from several experimental studies.[31,32] The multitude of conformational changes localized on the periphery or inside the blades will affect marginally the overall shape of the dendrimer. In contrast, more significant shape modifications may be favored by core conformation changes because these are associated with the overall movement of an entire blade (see below). Because the scope of this study is to investigate the overall shape changes of the dendrimer, rather than to explore the full conformational space, we will concentrate on the role played by the reciprocal orientation of the blades emerging from the core and generally disregard minor re-organizations occurring inside each blade.

To identify the plausible core conformations of planar 3-fold PDs, we notice that the pentasubstituted phenyl ring of each blade, directly bound to the 3-fold core, directs, toward the core, one phenyl ring on one side and a hydrogen atom on the other side of the connecting CC bond (see Figure 2a). We will take the position of these two groups in each blade as a reference for labeling the possible core-conformations. Optimization of both G1 and G2 structures (see below) indicates that this pentasubstituted phenyl is substantially rotated, with respect to the plane of PD's core, although it is not perpendicular to it. As a consequence, each blade can point the hydrogen above (Figure 2b,c) or below (Figure 2d,e) the core's plane, and because the pentasubstituted phenyl ring (practically the entire blade) is not perpendicular to the core's plane, the hydrogen can sit on the right or on the left with respect to this perpendicular.

By combining the four orientations shown in Figure 2b−e of two blades, we obtain the six possible reciprocal orientations shown in Figure 3: three are characterized by a true propeller (TP) orientation of the two blades and three by a nonpropeller (NP) orientation. The three TP arrangements may be distinguished by considering the groups (phenyl = P or hydrogen = H) confined in the region between the blades. Accordingly, in the top part of Figure 3 we have collected the TP(HP), TP(HH), and TP(PP) reciprocal orientations. Similarly, the three

TABLE 1: Summary of the Procedure Followed To Label Each of the Six Possible Core Conformations of Planar Three-Fold Core PDs

first pair of blades[a]	second pair of blades[a]	third pair of blades[a]		result[b]	core conformation[c]
TP(HP)	TP(HP)	TP(HP)	→	TP(HP−HP−HP)	TP(3HP)
NP(HP)	NP(HP)	TP(HP)	→	NP(HP−HP)TP(HP)	NP(2HP)
NP(HH)	TP(PP)	NP(HP)	→	NP(HP−HH)TP(PP)	NP(HH−HP)
NP(HH)	NP(PP)	TP(HP)	→	NP(HH−PP)TP(HP)	NP(HH−PP)
TP(HH)	TP(PP)	TP(HP)	→	TP(HH−PP−HP)	TP(MIX)
TP(HH)	NP(PP)	NP(HP)	→	NP(PP−HP)TP(HH)	NP(PP−HP)

[a] Reciprocal orientation assumed by the pair of blades; see the text for discussion and additional details in the Supporting Information section. [b] Short notation that summarizes the sequence of reciprocal orientations in the dendrimer. [c] Final label defining the resulting core conformation.

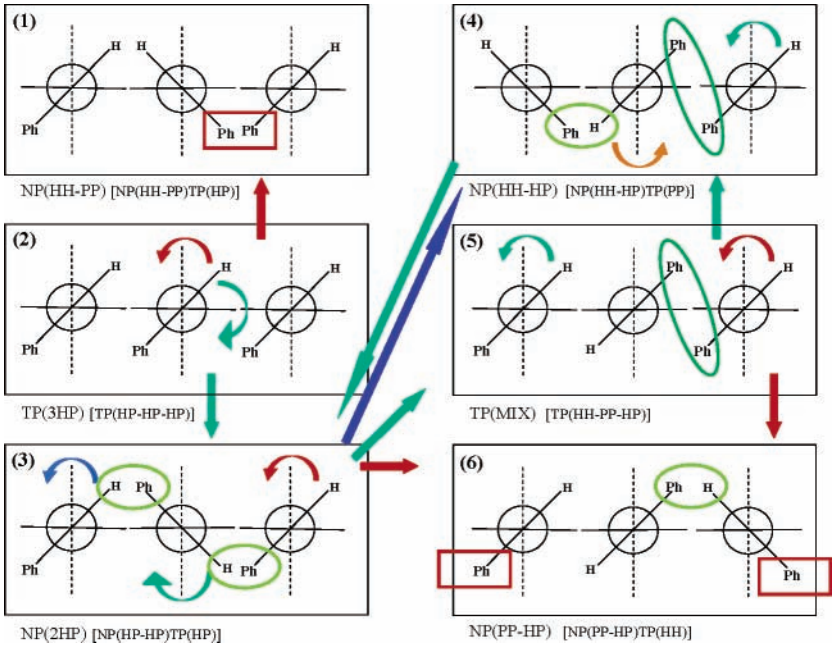

Figure 4. Schematic representation, in terms of Newman projections, and labeling of the six possible core conformations of planar 3-fold core PDs. Green circles indicate stabilizing interactions; red rectangles indicate destabilizing interactions. Green and blue arrows indicate possible paths for interconversion between stable core conformers, red arrows indicate possible paths for conversion to unstable core conformers, and finally, the orange arrow indicates a motion of one blade that does not change the core conformation state.

NP orientations can be distinguished by the P or H groups confined between the two blades and we obtain the NP(HP), NP(HH) and NP(PP) reciprocal orientations shown in the bottom part of Figure 3.

The reciprocal orientations of two blades can be unambiguously identified by monitoring the value of the two dihedral angles (for each pair of blades), indicated in the inset of Figure 1 (see also the Supporting Information section).

Combinations of the six reciprocal orientations leads to only six possible core conformations, as summarized in Table 1 and shown schematically in Figure 4. We have labeled each core conformation on the basis of the reciprocal orientations of the three pairs of blades. Notice that there are two core conformations in which the blades are all in a TP arrangement and four in which two pairs of blades are in a NP arrangement. The core conformer no. 2 in Figure 4 corresponds to the TP structure discussed in previous studies[18] and is characterized by three pairs of blades in the TP(HP) arrangement. Thus, we label this conformer as TP(3HP). In the second TP core conformer (no. 5 in Figure 4), all three possible TP arrangements of pairs of blades are present. For this reason we label it as TP(MIX). The remaining four core conformers, having two pairs of blades in a NP arrangement, are unambiguously identified by the sole sequence of the NP arrangements, and will be labeled, in the following, as NP(XX-YY) with XX, YY = HP, PP, HH. Two of these (nos. 1 and 6 in Figure 4), namely NP(HH−PP) and NP(PP−HP) are unstable, for this class of dendrimers, because of steric interactions. Indeed, they both contain a pair of blades in the NP(PP) arrangement, which implies a strong repulsion between the two phenyl groups confined between the blades (the repulsive interaction is schematically indicated, in Figure 4, by the red rectangles). The remaining two core conformers are the no. 3 and no. 4 in Figure 4, namely NP(HP−HP) or, shortly, NP(2HP) and NP(HH−HP). The NP(2HP) core conformer corresponds to the false-propeller structure discussed in previous studies.[18]

On the basis of the above-defined six core conformations, we have built six initial G1 and G2 dendrimer structures, with blades oriented accordingly. These initial geometries were optimized using the MM3 force field, to obtain starting structures for subsequent molecular dynamics simulations. As anticipated, two of the six core conformers, namely the NP(HH−PP) and NP(PP−HP) could not be optimized because of the strong steric repulsions and during energy minimization a jump to one of the remaining core conformations occurred. The remaining four core conformations were optimized for both G1 and G2 dendrimers and their energies are collected in Table 2. The equilibrium structures of both G1 and G2 core conformers are presented in Figure 5s and 6, respectively. Notice that each core conformer defined above corresponds to a collection of dendrimer's structures with the same core conformation but with different conformations of the phenyl rings that form each blade.

TABLE 2: MM3 Optimized Energies, Gyration Radius R_g, Characteristic Lengths ρ_1, ρ_2 and ρ_3, of the Four Stable Core Conformers of G1 and G2 Three-Fold Core PDs Employed as Initial Configurations in MD Simulations

core conformer	energy, kcal/mol	R_g, Å	ρ_1, Å	ρ_2, Å	ρ_3, Å
G1 TP(3HP)	77.1	7.1	2.7	4.5	4.7
G1 NP(2HP)	74.9	7.0	2.5	4.6	4.7
G1 TP(MIX)	78.1	7.0	2.7	4.4	4.8
G1 NP(HH−HP)	74.4	7.0	2.5	4.5	4.8
G2 TP(3HP)	206.2	12.2	3.6	7.8	8.6
G2 NP(2HP)	208.7	12.4	3.4	8.1	8.7
G2 TP(MIX)	202.7	12.1	2.8	6.1	10.0
G2 NP(HH−HP)	202.5	11.9	3.3	6.0	9.8

Thus, the energies listed in Table 2 and the structures shown in Figures 5 and 6 do not necessarily correspond to the lowest energy structures of a given core conformer. This is particularly evident for G2 dendrimers, for which a multitude of conformers with the same core arrangement exists.

The optimized structures are characterized, as anticipated, by blades twisted with respect to the core's plane. The twisting is, on average, larger for G1 structures than for G2 structures. In addition, G1 structures show a pseudo C_3 symmetry (see Figure 5), in that the three blades point approximately along the three C_2 axes of the C_3 symmetry point group. In other words, the overall shape of the four core conformations of G1 dendrimers can be defined as *open* in contrast with the *collapsed* shape assumed by two (the TP(MIX) and the NP(HH−HP)) of the four G2 core conformers, in which two blades have collapsed against each other (see Figure 6). Equilibrium structure calculations indicate that the collapse of two blades is induced by core-conformations with a pair of blades in the TP(PP) arrangement. Thus, in contrast with G1 dendrimers, G2 dendrimers can be classified as bistable because they may be found in two global shape's states: an *open* state if the core conformation is either TP(3HP) or NP(2HP) and a *collapsed* state if the core conformation is either TP(MIX) or NP(HH−HP). We will come back to this point in section 5, because MD simulations confirm more clearly the existence of these two global shape states for G2 dendrimers and show an oscillation between them.

To characterize more quantitatively the shapes associated with core conformations, we have calculated the eigenvalues of the gyration tensor (see section 2) for the optimized structures of the four stable core conformers of G1 and G2 PDs. The corresponding characteristic lengths and the gyration radius are collected in Table 2. It is seen that for G1 PDs two lengths (ρ_2 and ρ_3) are very similar whereas ρ_1 is substantially different and shorter, owing to the disklike shape of the dendrimer. For G2 dendrimers the ρ_1 length is shorter than the remaining two, and only slightly longer than the ρ_1 length of G1 dendrimers. The remaining two lengths are similar (both ca. 8 Å) for the two *open* conformers and substantially different (ca. 6 Å and 10 Å) for the two *collapsed* conformers. Thus, the characteristic lengths can be used to monitor global shape's changes occurring during MD simulations.

4. G1 Dendrimers

The energies listed in Table 2, corresponding to the four initial structures employed in the MD simulations, show that two core conformers (NP(2HP) and NP(HH−HP)) are more stable that the remaining two (TP(MIX), TP(3HP)). The NP(2HP) core conformer was indicated as the most stable G1 structure also in previous studies,[18] whereas here we identify a second core conformation (NP(HH−HP)) with a similar stability at 0 K.

4.1. Simulations at 80 K. The time evolution of the potential energy (PE) associated with the four MD simulations carried out at 80 K shows that, with the exception of the dynamics using the TP(MIX) initial structure, during the remaining three MD simulations the dendrimer remains in its initial core conformation (see also the Supporting Information section). The PE average values that can be extracted from the G1 dynamics are collected in Table 3 and correspond to the average energies at 80 K of the TP(3HP), NP(2HP) and NP(HP−HH) core conformers, respectively. The dynamics obtained from the TP(MIX) initial structure is slightly more complex, because the dendrimer switches immediately from the TP(MIX) to the NP(HH−HP) core conformation, and after about 3 ns it jumps to the NP(2HP) conformation. This is clearly seen in the top part of Figure 7, where the time evolution of the core conformation is followed by monitoring changes of the selected dihedral angles (see the inset of Figure 1).

The core conformation change is not associated with a global shape change, because all the four core conformers of G1 dendrimers are characterized by an *open* shape. As a result, the average gyration radius and the characteristic lengths listed in Table 3 are similar for the four MD simulations. Inspection of the time evolution of the characteristic lengths, shown in the bottom part of Figure 7, shows, indeed, that there is no appreciable change in these parameters before and after the conformation jump NP(HH−HP) → NP(2HP). As indicated in Figure 4, by green arrows, the observed core conformation jumps (TP(MIX) → NP(HH−HP) → NP(2HP)) require the twisting of a single blade without crossing the core's plane, namely, a motion characterized by a relatively small steric hindrance.

The average PEs listed in Table 3 indicate that the relative stability of the core conformers has changed, at 80 K, with respect to the values reported in Table 2 (minima on the PE surfaces, that is, energies at 0 K). In particular, we notice that at 80 K the NP(2HP) conformer is predicted to be more stable than the NP(HH−HP) conformer, by about 1.5 kcal/mol. Although this energy difference is relatively small, it is intriguing that their relative stability changes noticeably with the temperature. We can attempt to clarify qualitatively this peculiar behavior by analyzing the components of the total PE at 0 K and at 80 K. We can separate the energy components in bonding contributions (E_B) (stretching, bending, torsion, ...) and nonbonding contributions (E_{NB}) (wan der Waals and dipole−dipole). At 0 K, E_B is 64.9 kcal/mol for the NP(HH−HP) conformer and 68.5 kcal/mol for the NP(2HP) conformer, whereas the E_{NB} contributions are 9.5 and 6.4 kcal/mol, respectively. Thus, the comparable stability at 0 K arises from the balance between E_B and E_{NB}, with E_{NB} favoring the NP(2HP) conformer and the E_B favoring the NP(HH−HP) conformer. Average contributions at 80 K show that the E_{NB} terms are similar to those at 0 K, namely, 9.5 and 7.3 kcal/mol for the NP(HH−HP) and NP(2HP) conformers, respectively. Thus, the energy increase of the NP(HH−HP) conformer at 80 K is due to a larger temperature-induced destabilization of the remaining E_B contribution, with respect to that of the NP(2HP) conformer. The more favorable E_{NB} contribution for the NP(2HP) conformer, at 0 or 80 K, is connected with the stabilizing interaction between the hydrogen of one blade and the π-system of the phenyl [18] residing on the adjacent blade for each pair of NP(HP) arrangements (see the green circle in Figure 3 for the NP(HP) arrangement). Notice that, whereas the NP(2HP) core conformer is characterized by two of such interactions, the NP(HP−HH) core conformer is stabilized by only one (see Figure 4), which explains the less favorable E_{NB} contribution in the latter.

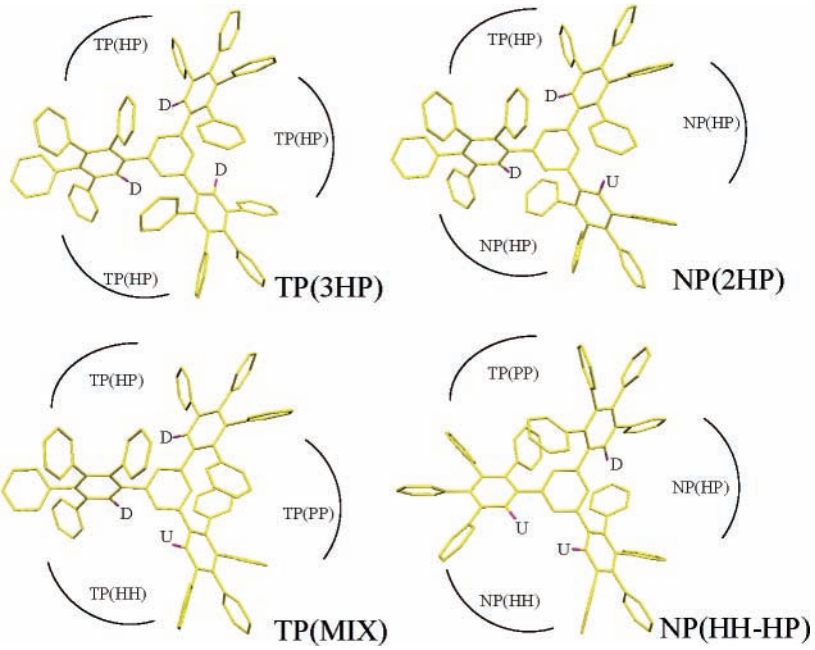

Figure 5. Optimized structures corresponding to the four stable core conformers of G1 PDs employed as initial configurations in MD simulations. Hydrogen atoms are omitted, except for the three hydrogens used to label the core conformations. The position (D = down, U = up) of these hydrogens, along with the reciprocal orientations of pair of blades, are indicated.

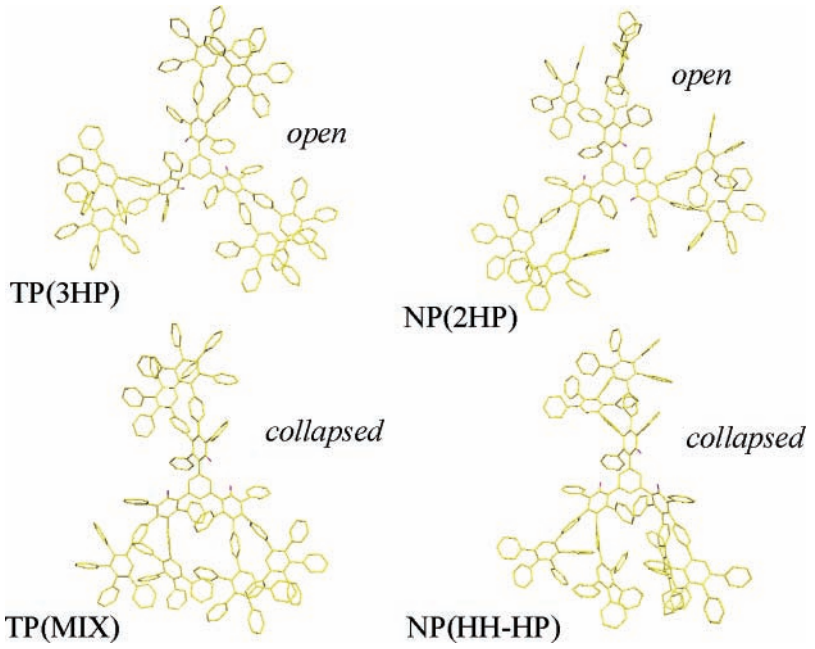

Figure 6. Optimized structures corresponding to the four stable core conformers of G2 PDs employed as initial configurations in MD simulations. Hydrogen atoms are omitted, except for the three hydrogens used to label the core conformations.

4.2. Simulations at 298 K. The time evolution of the PEs for the MD simulations carried out at 298 K shows a jump to lower energies can be identified only for the simulation using the TP(3HP) structure as initial configuration (see the Supporting Information). The remaining three simulations show oscillations around average values that are very similar in the three cases and also similar to the average energy in the second part of the simulation starting from the TP(3HP) configuration (see Table 3). A common average energy may indicate that the system evolves toward a unique, more favorable structure, or that the system jumps frequently among some structures of similar stability. To clarify this point, we have plotted (see Figure 8) the time dependent population of core conformation states for the four dynamics at 298 K. Inspection of Figure 8 shows that, at room temperature, jumps among core conformation states occur frequently. In particular, the simulations show that, generally, the NP(2HP) and the NP(HP−HH) conformers are more frequently populated than the TP(MIX) conformer and that the TP(3HP) conformer is populated only in the first 2.5 ns of the simulation starting from this core conformer. This behavior suggests that there must be a considerable barrier for the formation of the TP(3HP) conformer from the other three, which precludes its population. A possible explanation for such a barrier is that the formation of the TP(3HP) core conformer from the remaining three, requires a twisting of one blade through the core's plane, (see the green arrow in Figure 4 for

TABLE 3: Average Values of Energies, Gyration Radius and Characteristic Lengths ρ_1, ρ_2, ρ_3 from MD Simulations of G1 and G2 PDs, Carried out at 80 and 298 K

G1

	80 K					298 K				
initial core conformer	$\langle E\rangle$,[a] kcal/mol	$\langle R_g\rangle$, Å	$\langle\rho_1\rangle$, Å	$\langle\rho_2\rangle$, Å	$\langle\rho_3\rangle$, Å	$\langle E\rangle$, kcal/mol	$\langle R_g\rangle$, Å	$\langle\rho_1\rangle$, Å	$\langle\rho_2\rangle$, Å	$\langle\rho_3\rangle$, Å
TP(3HP)	113.6 ± 0.7 [TP(3HP)]	7.05 ± 0.02	2.6 ± 0.1	4.53 ± 0.07	4.72 ± 0.06	220.8 ± 2.6 − 218.8[e] ± 2.7	7.04 ± 0.04	2.6 ± 0.2	4.5 ± 0.1	4.8 ± 0.1
NP(2HP)	111.3 ± 0.7 [NP(2HP)]	7.05 ± 0.02	2.6 ± 0.1	4.56 ± 0.06	4.73 ± 0.04	218.3 ± 2.7	7.04 ± 0.04	2.6 ± 0.2	4.5 ± 0.1	4.7 ± 0.1
TP(MIX)	112.7 ± 0.8 [NP(HH−HP)][b] 111.3 ± 0.6 [NP(2HP)][b]	7.04 ± 0.02	2.6 ± 0.1	4.54 ± 0.06	4.74 ± 0.06	218.9 ± 2.8	7.04 ± 0.04	2.6 ± 0.2	4.5 ± 0.1	4.8 ± 0.1
NP(HH−HP)	112.8 ± 0.8 [NP(HH−HP)]	7.04 ± 0.02	2.5 ± ±0.1	4.53 ± 0.07	4.75 ± 0.06	218.7 ± 2.6	7.04 ± ±0.04	2.6 ± 0.2	4.5 ± 0.1	4.8 ± 0.1

G2

	80 K					298 K				
initial core conformer	$\langle E\rangle$,[a] kcal/mol	$\langle R_g\rangle$, Å	$\langle\rho_1\rangle$, Å	$\langle\rho_2\rangle$, Å	$\langle\rho_3\rangle$, Å	$\langle E\rangle$,[α] kcal/mol	$\langle R_g\rangle$, Å	$\langle\rho_1\rangle$, Å	$\langle\rho_2\rangle$, Å	$\langle\rho_3\rangle$, Å
TP(3HP)	316.5 ± 1.2 [TP(3HP)]	12.1 ± 0.1	3.0 ± 0.1	7.9 ± 0.5	8.7 ± 0.3	622.6 ± 5.6	12.1 ± 0.2	3.5 ± 0.4	7.1 ± 0.8	9.2 ± 0.4
NP(2HP)	317.7 ± 1.2 [NP(2HP)][c]	12.2 ± 0.1	3.1 ± 0.3	7.7 ± 0.4	9.0 ± 0.3	621.8 ± 5.2	12.0 ± 0.2	3.5 ± 0.4	6.7 ± 0.6	9.4 ± 0.4
TP(MIX)	313.1 ± 1.0 [TP(MIX)][d] 309.9 ± 1.1 [NP(HP−HH)][d]	12.01 ± 0.06[d] 11.74 ± 0.07[d]	2.8 ± 0.1[d] 3.3 ± 0.1[d]	6.2 ± 0.1[d] 5.1 ± 0.1[d]	9.9 ± 0.1[d] 10.1 ± 0.1[d]	623.0 ± 5.1	12.2 ± 0.2	3.5 ± 0.4	7.4 ± 0.7	9.0 ± 0.4
NP(HH−HP)	314.0 ± 1.1− 312.8 ± 1.1 [NP(HH−HP)]	11.84 ± 0.05	3.40 ± 0.08	5.7 ± 0.1	9.82 ± 0.08	625.0 ± 4.8	12.2 ± 0.2	3.7 ± 0.4	7.3 ± 0.7	9.0 ± 0.4

[a] The average energy is followed, in parentheses, by the core conformer to which it corresponds. [b] The first value is the average over the first 3 ns, the second value is the average over the last nanosecond, that is, before and after the core conformation jump (see the discussion in the text). [c] Average computed in the 0.8−4 ns time range, that is, after the PE decrease (see Figure 9 and the discussion in the text). [d] The first value is the average over the first 1.4 ns, the second value is the average in the 1.5−4 ns time range, that is, before and after the TP(MIX) → NP(HH−HP) core conformation jump (see Figure 9 and the discussion in the text). [e] The first value is the average over the first 2.2 ns, the second value is the average in the 2.4−8 ns time range, that is, before and after the TP(3HP) → (NP(2HP);NP(HH−HP)) conformation jump (see the discussion in the text).

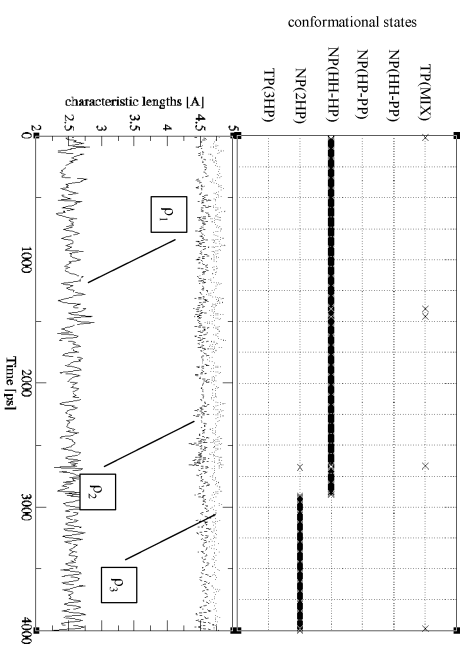

Figure 7. Analysis of the simulation ($T = 80$ K, G1 dendrimer) carried out with the TP(MIX) initial configuration. (Top) time evolution of the population of core conformational states. The initial TP(MIX) configuration converts immediately to the NP(HH−HP) core conformation and later, after ca. 2.9 ns, the NP(HH−HP) → NP(2HP) jump occurs. (Bottom) time evolution of the characteristic lengths ρ_1, ρ_2 and ρ_3 showing that the global shape is conserved during the simulation.

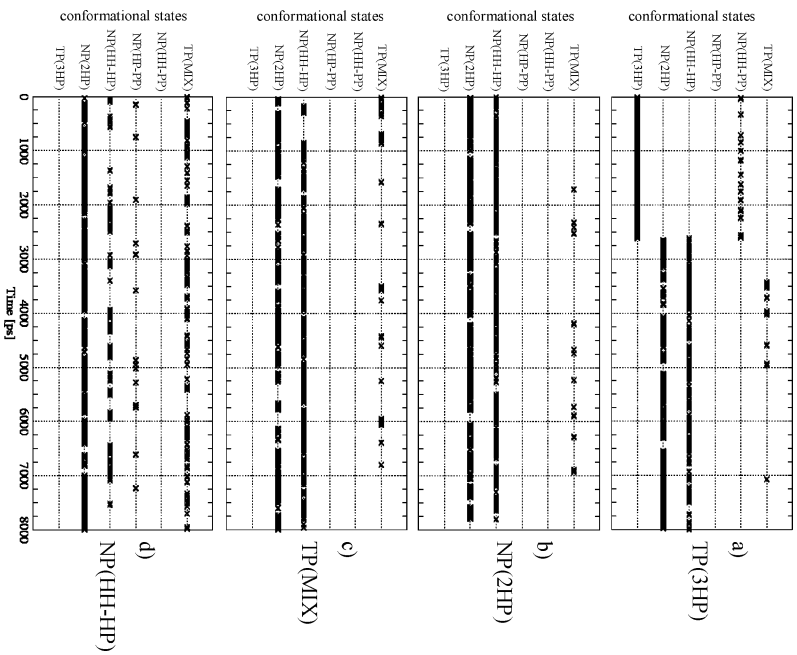

Figure 8. Time evolution of the population of core conformational states for the simulations carried out at 298 K (G1 dendrimers): (a) simulation using the core conformer TP(3HP) as the initial configuration; (b) simulation using the core conformer NP(2HP) as the initial configuration; (c) simulation using the core conformer TP(MIX) as the initial configuration; (d) simulation using the core conformer NP(HH−HP) as the initial configuration.

the TP(3HP) → NP(2HP) jump) a motion which is associated with remarkable steric interactions between blades.

Similarly to the simulations carried out at low temperature, the G1 dendrimer conserves an *open* shape during the room-temperature dynamics, and the time evolution of its characteristic lengths shows modest oscillations around the average values

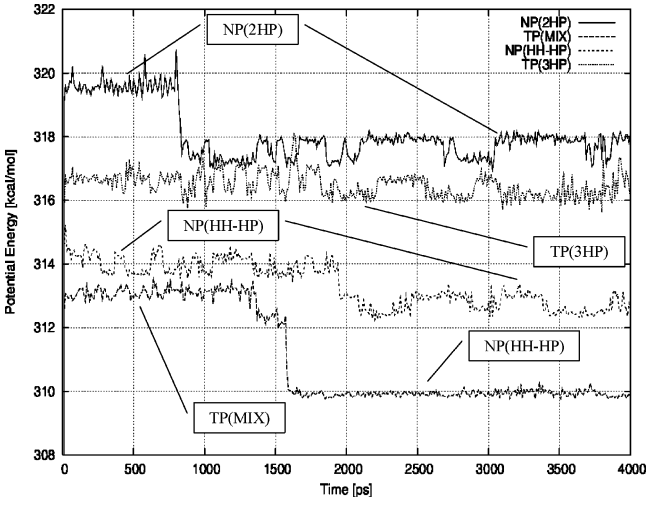

Figure 9. Time evolution of the potential energy from NVT MD simulations, $T = 80$ K, carried out on isolated G2 dendrimers. The initial configuration for each of the four simulations is indicated in the top right angle of the figure. The core conformers sampled during each dynamics are also indicated.

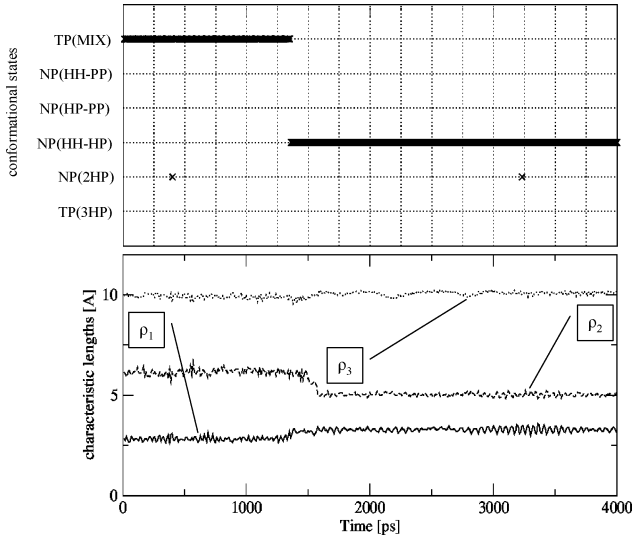

Figure 10. Analysis of the simulation ($T = 80$ K, G2 dendrimer) carried out with the TP(MIX) initial configuration. (Top) time evolution of the population of core conformational states. The initial TP(MIX) configuration converts, after ca. 1.4 ns, to the NP(HH−HP) core conformer. (Bottom) time evolution of the characteristic lengths ρ_1, ρ_2 and ρ_3 showing that a global shape's change is associated with the TP(MIX) → NP(HH−HP) core conformation jump.

listed in Table 3. As expected, these are very similar for all the four simulations.

In summary, simulations on G1 dendrimers show that they are globally shape persistent at low and room temperature, although at room temperature core conformation jumps occur very frequently among three of the four accessible core conformers. In other words, the global shape of G1 dendrimers is temperature independent.

5. G2 Dendrimers

As described above, MD simulations were carried out using, as initial configurations, the four core conformations shown in Figure 4 whose energies are listed in Table 2. The more stable initial structure is predicted to be the NP(HH−HP), but as discussed in section 3, the energies in Table 2 do not necessarily correspond to the lowest energy for each core conformer. However, we notice that two groups of core conformers (the TP(MIX) and NP(HH−HP)) have energies markedly lower than the other two (NP(2HP) and TP(3HP)). The energy difference between these two groups, (ca. 3−6 kcal/mol; see Table 2) is similar to the *open-club shape* energy difference computed from UFF simulations.[18] On the basis of our computed energy differences, we can state with confidence that, at 0 K, the lowest energy core conformations are either the TP(MIX) or the NP-(HH−HP). The rationale behind this computed result is easily understood by inspecting the dominant stabilizing interactions (green circles) schematically indicated in Figure 4 for each core conformer. These are the already mentioned hydrogen−phenyl interaction in the NP(HP) arrangement along with the attraction between two blades, which leads to a *collapsed* structure and which is favored by the TP(PP) arrangement. Figure 4 shows that the TP(PP) stabilizing arrangement occurs in both the TP(MIX) and the NP(HH−HP) core conformers, with the latter conformer further stabilized by the presence of a NP(HP) arrangement. Thus, it can be expected that, for G2 PDs, the NP(HH−HP) core conformer corresponds to the most stable dendrimer structure. Notice that, in contrast, the TP(PP) arrangement does not stabilize G1 dendrimers because of the reduced dimension of the blades, which is not compatible with collapsing.

5.1. Simulations at 80 K. In Figure 9 we present the time evolution of the PEs for the four MD simulations carried out at 80 K. It is seen that jumps to lower energies are computed for three out of four simulations. The simulation starting from the NP(2HP) core conformer shows a jump to lower energies (by about 2 kcal/mol) after about 900 ps, and subsequently the PE remains stable. The PE extracted from the MD simulation that used the NP(HH−HP) conformation as initial configuration shows a less marked jump (of about 1 kcal/mol) after ca. 2 ns and, finally, the PE of the MD started with the TP(MIX) core conformer shows a clear and remarkable jump (about 3 kcal/mol) after ca. 1.5 ns.

To clarify the nature of the structural changes that determine the PE decreases, we can inspect the time dependent population of core conformation states in the top part of Figure 10, which shows that only for the MD started from the TP(MIX) core conformer, a jump to another core conformer occurs. The core conformation change can be easily appreciated by inspecting the time evolution of ρ_1, ρ_2 and ρ_3 shown in the bottom part of Figure 10: a discontinuity in the characteristic lengths is observed after the core conformation jump. However, ρ_2 and ρ_3 remain substantially different, which implies that the new core conformer is still characterized by a *collapsed* global shape. Indeed, the jump occurs between the TP(MIX) and the NP(HH−HP) conformers, both characterized (as discussed in section 3) by the presence of a TP(PP) pair of blades favoring the *collapsed* shape.

In the remaining three MD simulations, core conformation jumps do not occur, and thus the computed energy stabilization must be associated with structural rearrangements internal to the blades. Inspection of the time evolution of the characteristic lengths (see Figure 11) shows substantial variations only for the simulation started from the NP(2HP) and the TP(3HP) core conformers. For the NP(2HP) conformer, the sudden energy lowering observed in Figure 9 is accompanied by a slight change in ρ_1 and a more remarkable change in the periodic behavior of ρ_2 and ρ_3.

The oscillations of ρ_2 and ρ_3 suggest that the dendrimer is attempting an *open* → *collapsed* global shape change, without success. Indeed, the two lengths remain in a range compatible with *open* structures and thus, as anticipated in section 3, the

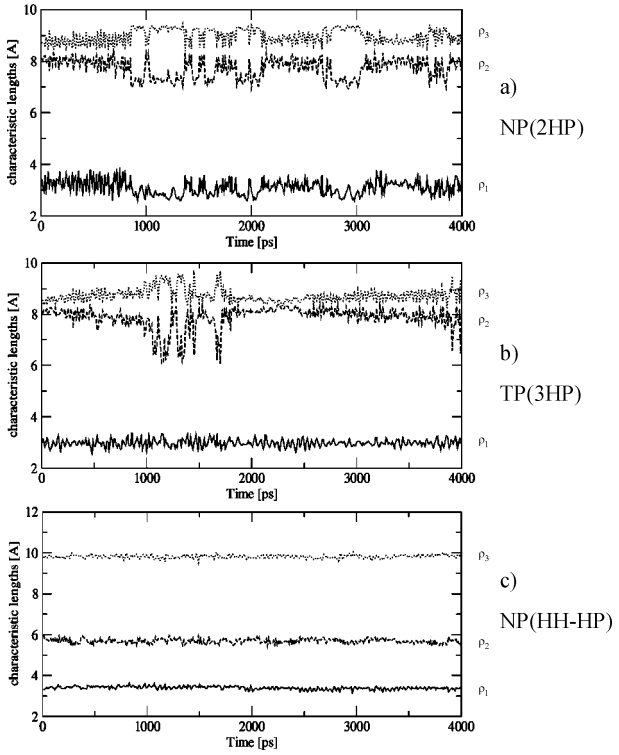

Figure 11. Time evolution of the characteristic lengths ρ_1, ρ_2 and ρ_3 for the simulations (T = 80 K, G2 dendrimer) carried out with (a) NP(2HP) initial configuration, (b) TP(3HP) initial configuration, and (c) NP(HH−HP) initial configuration.

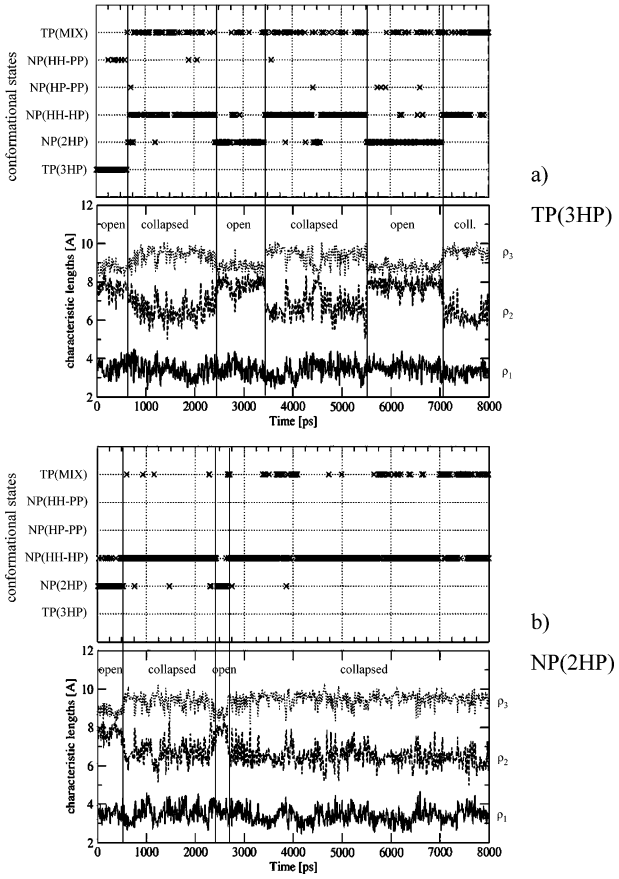

Figure 12. (a) MD simulation (T = 298 K, G2 dendrimer) carried out with the TP(3HP) initial configuration. (a, Top) time evolution of the population of core conformational states and (a, bottom) time evolution of the characteristic lengths ρ_1, ρ_2 and ρ_3. Core conformation jumps are associated with global shape's changes as indicated. (b) Same analysis as above for the simulation carried out with the NP(2HP) initial configuration.

MD simulation shows that the NP(2HP) core conformer is always associated with an *open* global shape. The structural reorganization occurring during the MD at 80 K leads, however, to a more stable NP(2HP) core conformer. Indeed, geometry optimization of a structure sampled at the end of the simulation gives an energy of 206.8 kcal/mol, to be compared with the initial 208.7 kcal/mol configuration (see Table 2).

The ρ_1, ρ_2 and ρ_3 time evolution for the TP(3HP) core conformer is similar to that of the NP(2HP) core conformer; that is, it shows an oscillatory behavior of ρ_2 and ρ_3, which suggests frustrated attempts to convert to a more stable *collapsed* structure. In contrast, the almost negligible oscillation of the three lengths during the MD started from the NP(HH−HP) core conformer is justified by its already stable *collapsed* shape. The dendrimer has too little energy at 80 K to change its global shape during the MD simulation, and the energy decrease observed after ca. 2 ns is due to minor structural rearrangements. Interestingly, the simulations started from the TP(MIX) and the NP(HH−HP) core conformers lead to equilibrated structures both belonging to the ensemble of NP(HH−HP) core conformers. However, the two equilibrated NP(HH−HP) core conformers are not identical, as indicated by their different average energies (see Table 3) and by the optimized energies of two structures sampled from the two simulations (199.5 and 200.8 kcal/mol), both lower than that of the initial NP(HH−HP) core conformer listed in Table 2.

In summary, these simulations indicate that core conformation jumps are rare at 80 K, although minor structural rearrangements may occur. As a consequence, the global shape is conserved at this temperature and the lowest energy core conformer is found to be the NP(HH−HP), owing to the stabilizing contribution of TP(PP) and NP(HP) blade's arrangements.

5.2. Simulations at 298 K. The average PEs extracted from the four simulations carried out at 298 K are collected in Table 3. The time dependent population of core conformational states along with the time evolution of the characteristic lengths are depicted in Figure 12 for the dynamics using TP(3HP) and NP(2HP) initial configurations and in Figure 13 for the dynamics using the TP(MIX) and NP(HH−HP) initial configurations. Similar to the G1 dendrimers, jumps among the core conformation states of G2 dendrimers occur at room temperature, although less frequently than for the G1 dendrimers. The simulations show that, generally, the NP(2HP) and the NP(HH−HP) conformers are more populated than the TP(MIX) conformer and that the TP(3HP) conformer is populated only in the first 0.7 ns of the simulation starting from this core conformer. Thus, the population of core conformers for G2 dendrimers follows the same trend already discussed for G1 PDs. The barriers for the formation of the TP(3HP) conformer from the other three are likely to be even larger in this case, owing to the larger dimension of the dendrimer's blade that must cross the core's plane. Similarly to the simulations carried out at low temperature, the major characteristic of G2 dendrimers is their global shape, which can be either *open* or *collapsed*. The comparison between the sequence of conformational state jumps and the evolution of the ρ_2 and ρ_3 characteristic lengths during each simulation (see Figures 12 and 13) shows clearly that the global shape of the dendrimer changes in parallel with the core conformation jumps. Inspection of Figures 12 and 13 shows that, invariably, ρ_2 and ρ_3 converge to similar values when the G2 dendrimer is in either the TP(3HP) or NP(2HP) core

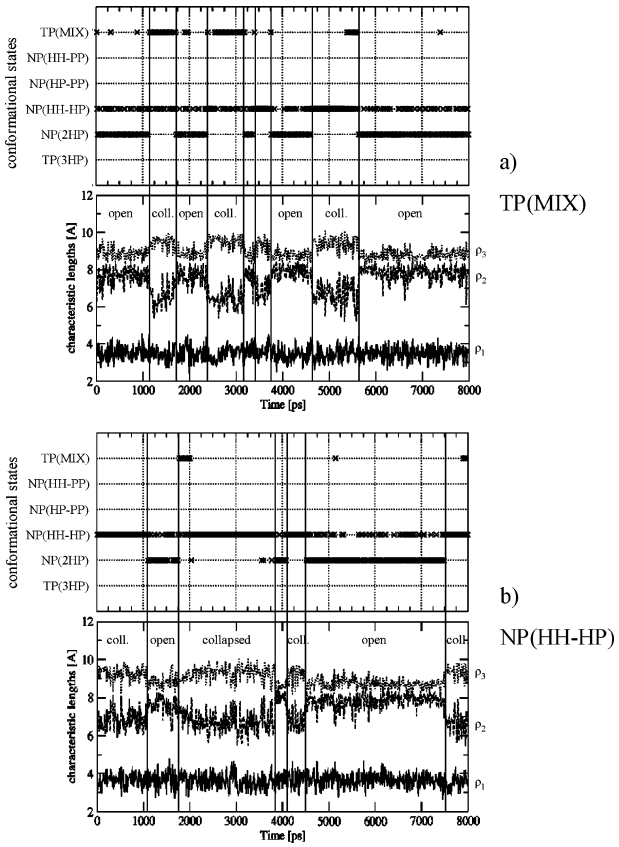

Figure 13. (a) MD simulation ($T = 298$ K, G2 dendrimer) carried out with the TP(MIX) initial configuration. (a, Top) time evolution of the population of core conformational states and (a, bottom) time evolution of the characteristic lengths ρ_1, ρ_2 and ρ_3. Core conformation jumps are associated with global shape's changes as indicated. (b) Same analysis as above for the simulation carried out with the NP(HH−HP) initial configuration.

conformation, whereas they diverge to substantially different values when the dendrimer jumps to the TP(MIX) or NP(HH−HP) core conformations. We notice that the *open* and *collapsed* structures found in the present study are very similar to those found by Brocorens et al.[18]

Conversely, the structures found here are remarkably different from the flowerlike structures found in ref 20 for the same G2 dendrimer. In contrast with the results of ref 18, we do not see, at room temperature, a decay of the G2 dendrimer from an *open* to a *collapsed* structure, but an oscillation between the two global shapes, owing probably to the longer simulation time of this study. The oscillation between two global shape's states, seen here for the first time, confirms the hypothesis proposed in ref 18 that interconversion between conformers might occur. The four simulations discussed above show that the dendrimer retains a given global shape (either *open* or *collapsed*) for a time in the range of nanoseconds.

In summary, nanosecond MD simulations on G2 dendrimers at 80 K, do not show changes of the global shape. Increasing the temperature to 298 K leads to frequent core conformation jumps occurring in the nanosecond time range and associated with an oscillatory *open* ↔ *collapsed* global shape's change that can be monitored by following the evolution of the characteristic lengths ρ_2 and ρ_3.

6. Conclusions

We have presented a computational study on the properties of a recently synthesized class of dendritic systems formed only by carbon and hydrogen atoms. These planar 3-fold core PDs may be found, generally, in either an *open* or a *collapsed* global shape state. Although G1 PDs exist only in the *open* state, starting from G2 dendrimers, the two global shape states may be observed.

We have proposed a classification of the core conformers of these planar 3-fold core dendrimers that allows us to rationalize the existence of the two global shapes adopted by the higher generation dendrimers.

The classification is based on the reciprocal orientations of pairs of dendrons which lead to stabilizing or destabilizing interactions. Only six core conformations can exist for these dendrimers and only four stable core conformations are identified by computations, along with the ease or difficulty of interconversion between them. In the case of G2 dendrimers, two of the four stable core conformers are associated with an *open* global shape and two with a *collapsed* global shape. We can generalize this observation by concluding that each global shape state (either *open* or *collapsed*) is associated with a precise collection of core conformations.

In particular, it has been shown that collapsing of two dendrons is induced by a specific reciprocal orientation of two blades, namely the TP(PP) arrangement, which favors their nonbonding interaction. Such collapsing does not occur in G1 dendrimers owing to the small size of their dendrons, whereas for G2 (and higher generation) dendrimers, the collapse of two dendrons results in a stabilization.

The stabilizing attraction between *collapsed* dendrons induced by the presence of a TP(PP) arrangement explains why the NP(2HP) and NP(HH−HP) core conformations have similar stability for G1 dendrimers, whereas the energy of the NP(HH−HP) core conformation becomes remarkably lower for G2 dendrimers. For higher generation dendrimers it may be expected that the *collapsed* state will be even more stabilized as compared with the *open* state.

MD simulations in the nanosecond time range at 80 K show that G1 and G2 dendrimers conserve their initial shape. The persistence of the global shape at low temperature suggests that, among other possible uses, these dendrimers should be able to trap small molecules in intra- or intermolecular cavities and work in this direction is in progress.

The MD carried out at room temperature indicate that core conformation jumps occur frequently. Although these conformation changes have little effect on the global shape of G1 dendrimers, for G2 dendrimers they imply a bistability because reversible oscillations between the two global shape states (*open* and *collapsed*) are observed during the MD simulations.

Because the frequency of core conformation jumps decreases from G1 to G2 dendrimers (at room temperature) we expect a further frequency decrease for higher generation dendrimers. As a consequence, larger dendrimers are expected to conserve their global shape (*open* or *collapsed*) for several nanoseconds at 298 K. Furthermore, this study shows that the generation of the dendrimer may influence the predominance of one of the two global shape's states. Although the *open* state is dominant for G1 dendrimers, the *collapsed* state is likely to become dominant for generations above G2. G2 dendrimers at room temperature seem to represent the best combination of dendrimer size and thermodynamical conditions for observation of bistability. In this sense this computational study suggests that it might be possible to tune the time-range in which the *open* ↔ *collapsed* transition occurs by selecting the appropriate temperature and size of the dendrimer. Because the results discussed here were obtained by neglecting intermolecular interactions,

the combination dendrimer size and ambient conditions along with the occurrence of bistability cannot be directly extrapolated to the condensed phase. These isolated molecule simulations, however, can be considered representative of a poor solvent environment.

It can be concluded that the rigid shape of the dendrimers investigated in this work might favor, especially at low temperature, the formation of stable intramolecular or intermolecular cavities able to accommodate small molecules. At the same time, the computed bistability of their global shape suggests that, in some cases, the trapping might be switched on and off by forcing the *open* ↔ *collapsed* transition. Aside from trapping, other functionalities might be imagined for these dendrimers, taking advantage of this bistability: for instance chemical functionalization[33] of the dendrons with specific chromophores might be employed to photoinduce the *open* ↔ *collapsed* transition, etc.

The computed bistability appears to be an interesting property of this class of PDs but is discussed here on the basis of isolated molecule simulations. Higher generation dendrimers, other classes of PDs and solvent and/or aggregation effects will be the subject of future studies.

Acknowledgment. This work was supported by funds from MIUR (grant 60%), from MURST Cofin 2004 (project: "Spettroscopia rotazionale in assorbimento e a trasformate di Fourier: Produzione e studio di nuovi cluster e specie molecolari in espansioni supersoniche"), and from FIRB 2001 (project: "Carbon based micro and nanostructures", RBNE019NKS). Support by the German Science Foundation (SFB 625) is also gratefully acknowledged. We are indebted to Dr. Chris Clark for useful discussions.

Supporting Information Available: 6 pages including: (1) definition of the new atom types, including one figure (Figure S1) and one table (Table S1) containing the additional force field parameters employed in the MD simulations; (2) one table (Table S2) containing the range of dihedral angles that define the six possible reciprocal orientations of dendrimer's blades; (3) two figures (Figure S2, Figure S3) representing the time evolution of the potential energy during the MD simulations of G1 dendrimers at 80 K and at room temperature. This material is available free of charge via the Internet at http://pubs.acs.org.

References and Notes

(1) Fischer, M.; Vogtle, F. *Angew. Chem., Int. Ed.* **1999**, *38*, 885−905.

(2) Reetz, M. T.; Lohmer, G.; Schwickari, R. *Angew. Chem., Int. Ed. Engl.* **1997**, *36*, 1526−1529.

(3) Jockusch, S.; Ramirez, J.; Sanghvi, K.; Nociti, R.; Turro, N. J.; Tomalia, D. A. *Macromolecules* **1999**, *32*, 4419−4423.

(4) Qu, J. Q.; Pschirer, N. G.; Liu, D. J.; Stefan, A.; De Schryver, F. C.; Mullen, K. *Chem.-Eur. J.* **2004**, *10*, 528−537.

(5) Balzani, V.; Campagna, S.; Denti, G.; Juris, A.; Serroni, S.; Venturi, M. *Acc. Chem. Res.* **1998**, *31*, 26−34.

(6) Halim, M.; Pillow, J. N. G.; Samuel, D. W.; Burn, P. L. *Adv. Mater.* **1999**, *11*, 371−374.

(7) Zhao, M. Q.; Crooks, R. M. *Angew. Chem., Int. Ed.* **1999**, *38*, 364−366.

(8) Newkome, G. R.; Moorefield, C. N.; Vogtle, F. *Dendritic Molecules*; VCH Verlag: Weinheim, 1996.

(9) Berresheim, A. J.; Muller, M.; Mullen, K. *Chem. Rev.* **1999**, *99*, 1747−1785.

(10) Morgenroth, F.; Reuther, E.; Mullen, K. *Angew. Chem., Int. Ed. Engl.* **1997**, *36*, 631−634.

(11) Morgenroth, F.; Berresheim, A. J.; Wagner, M.; Mullen, K. *Chem. Commun.* **1998**, 1139−1140.

(12) Watson, M. D.; Fechtenkotter, A.; Mullen, K. *Chem. Rev.* **2001**, *101*, 1267−1300.

(13) Simpson, C. D.; Mattersteig, G.; Martin, K.; Gherghel, L.; Bauer, R. E.; Rader, H. J.; Mullen, K. *J. Am. Chem. Soc.* **2004**, *126*, 3139−3147.

(14) Di Stefano, M.; Negri, F.; Carbone, P.; Müllen, K. *Chem. Phys.* **2005**, *314*, 85−99.

(15) Morgenroth, F.; Kubel, C.; Muller, M.; Wiesler, U. M.; Berresheim, A. J.; Wagner, M.; Mullen, K. *Carbon* **1998**, *36*, 833−837.

(16) Percec, V.; Ahn, C. H.; Ungar, G.; Yeardley, D. J. P.; Moller, M.; Sheiko, S. S. *Nature* **1998**, *391*, 161−164.

(17) Morgenroth, F.; Kubel, C.; Mullen, K. *J. Mater. Chem.* **1997**, *7*, 1207−1211.

(18) Brocorens, P.; Zojer, E.; Cornil, J.; Shuai, Z.; Leising, G.; Mullen, K.; Bredas, J. L. *Synth. Met.* **1999**, *100*, 141−162.

(19) Wind, M.; Wiesler, U. M.; Saalwachter, K.; Mullen, K.; Spiess, H. W. *Adv. Mater.* **2001**, *13*, 752−756.

(20) Pricl, S.; Fermeglia, M.; Ferrone, M.; Asquini, A. *Carbon* **2003**, 41, 2269−2283.

(21) http://www.accelrys.com/.

(22) Rappe, A. K.; Casewit, C. J.; Colwell, K. S.; Goddard, W. A.; Skiff, W. M. *J. Am. Chem. Soc.* **1992**, *114*, 10024−10035.

(23) Sun, H. *J. Phys. Chem. B* **1998**, *102*, 7338−64.

(24) Allinger, N. L.; Yuh, H. Y.; Lii, J. H. *J. Am. Chem. Soc.* **1989**, *111*, 8551−66.

(25) Ponder, J. W. In *TINKER, Software Tools for Molecular Design version 3.8*, 1990−2003; pp http://dasher.wustl.edu/tinker.

(26) Allinger, N. L.; Lii, J. H. *J. Comput. Chem.* **1987**, *8*, 1146−1153.

(27) Almond, A.; Axelsen, J. B. *J. Am. Chem. Soc.* **2002**, *124*, 9986−9987.

(28) Šolc, K.; Stockmayer, W. H. *J. Chem. Phys.* **1971**, *54*, 2756−2757.

(29) Theodorou, D. N.; Suter, U. W. *Macromolecules* **1985**, *18*, 1206−1214.

(30) Berendsen, H. J. C.; Postma, J. P. M.; van Gusteren, W. F.; Di Nola, A.; Haak, J. R. *J. Chem. Phys.* **1984**, *81*, 3684−3690.

(31) Loi, S.; Wiesler, U. M.; Butt, H. J.; Mullen, K. *Macromolecules* **2001**, *4*, 3661−3671.

(32) Wind, M.; Saalwachter, K.; Wiesler, U. M.; Mullen, K.; Spiess, H. W. *Macromolecules* **2002**, *35*, 10071−10086.

(33) Grebel-Koehler, D.; Liu, D. J.; De Feyter, S.; Enkelmann, V.; Weil, T.; Engels, C.; Samyn, C.; Mullen, K.; De Schryver, F. C. *Macromolecules* **2003**, *36*, 578−590.